Dendritic Physical Gels: Structural Parameters for Gelation with Peptide-Core Dendrimers

Woo-Dong Jang and Takuzo Aida*

Department of Chemistry and Biotechnology, School of Engineering, The University of Tokyo, 7-3-1 Hongo, Bunkyo-ku, Tokyo 113-8656, Japan

Received February 20, 2003; Revised Manuscript Received June 28, 2003

ABSTRACT: Eleven different peptide-core dendritic macromolecules, each having a [G2] poly(benzyl ether) dendritic wedge (Den) at the peptide side chain, N-terminal, or C-terminal, were synthesized, and their potentials as macromolecular organic gelators were investigated in MeCN. Among these candidates, side-chain-dendronized Boc-Tyr(Den)-Ala and cyclo-(Tyr(Den)-Ala) and N-dendronized Den-Phe-Ala and Den-Phe-Ala-OMe (Figure 1) were found to form physical gels with critical concentrations for gelation of 1.0−2.2 mM, whereas C-dendronized Boc-Phe-Ala-ODen and Phe-Ala-ODen were unable to induce gelation. FE-SEM micrographs of the dry gels showed the presence of fibrous or ribbonlike self-assembled structures, which melted at 112−214 °C (T_m), depending on the modes of hydrogen bonding and van der Waals interactions. Infrared spectroscopy and X-ray diffraction analysis of the dry gels indicated columnar molecular orderings with a rectangular packing geometry for Boc-Tyr(Den)-Ala and Den-Phe-Ala-OMe, while a lamellar geometry for Den-Phe-Ala. Circular dichroism analysis of the transparent gel with Boc-Tyr(Den)-Ala indicated a helically twisted geometry of hydrogen-bonded dipeptide arrays.

Introduction

Dendrimers are nanoscopic hyperbranched macromolecules with well-predictable three-dimensional shapes, and they are potential candidates for the bottom-up strategy for the fabrication of supramolecular functional materials.[1,2] As the driving forces for the self-organization of dendritic macromolecules, a variety of interactions such as hydrogen-bonding,[3] metal-ligating,[4] metal ion−metal ion,[5] van der Waals,[6] and electrostatic interactions[7] have been utilized. In a previous communication,[8] we have reported the first example of dendritic physical gel using an ester-terminated poly(benzyl ether) dendron with a dipeptide focal core (Boc-Tyr(Den)-Ala; Figure 1), where a hierarchical self-organization takes place to form a micrometer-scale fibrous assembly of nanometer-scale subelementary dendritic fibrils. Later, several new examples that form dendritic physical gels have been reported. For instance, Majoral and co-workers have reported organophosphorus dendrimers as excellent gelators for water, to form functional hydrogels.[9] Smith and co-workers have reported physical gelation of organic solvents with polylysine dendrimers triggered by diamines.[10] On the other hand, Kim and co-workers have found that certain polyamine dendrimers form physical gels in organic solvents, while they form vesicles in aqueous media.[11] Thus, one may note a divergent growth of the research field focusing on dendritic physical gels.

Although ordinary gelling agents carry long alkyl chains in combination with hydrogen-bonding modules for the unidirectional growth of self-organized structures, the dendritic gelators so far reported[8−10] do not require long alkyl chains. Therefore, it should be interesting to investigate structural parameters of dendritic macromolecules to dominate their gelation properties. We have already shown that the efficient gelation with Boc-Tyr(Den)-Ala requires a large [G2] or [G3] poly(benzyl ether) dendritic wedge (Den), where the critical concentration for gelation is as low as 1.0 mM.[8] In contrast, lower-generation homologues do not form gels but only give a crystalline solid. In other to obtain structural parameters as required for the efficient gelation, we newly synthesized a series of 10 different peptide-core dendritic macromolecules with a [G2] poly(benzyl ether) dendritic wedge and investigated in MeCN their potentials as macromolecular organic gelators. In particular, we wish to highlight a significant effect of the topology of the dendritic wedge on the self-assembling mode.

* Corresponding author. E-mail: aida@macro.t.u-tokyo.ac.jp.

Experimental Section

Preparation of Dendritic Macromolecules: Chemicals. Dipeptides used as the core modules (Figure 2) were prepared according to conventional methods for peptide synthesis. All other reagents were used as received from commercial sources (TCI, Aldrich). Solvents were freshly distilled according to literature methods.

2d (Figure 2)**.** A tetrahydrofuran (THF) solution (5 mL) of a mixture of 3,5-bis(4-methoxycarbonylbenzyloxy)benzyl bromide (2.0 mmol) and trichloroethyl 3,5-dihydroxybenzoate (0.91 mmol), containing K_2CO_3 (2.45 mmol) and 18-crown-6 (1.24 mmol), was refluxed under Ar for 48 h. The reaction mixture was then evaporated to dryness, and the residue was chromatographed on silica gel with CH_2Cl_2/hexane (75/25) as eluent, where the first fraction was collected and freeze-dried from benzene to give **2d** (0.67 mmol) as a white solid in 74% yield. MALDI−TOF-MS for $C_{59}H_{51}Cl_3O_{16}$ *m/z*: calcd, 1122 [M+]; found, 1122. ^{1}H NMR ($CDCl_3$): δ 3.90 (s, 12H; dendron CO_2-CH_3), 4.92 (s, 2H; OCH_2CCl_3), 5.00 and 5.08 (s, 12H; OCH_2-Ar), 6.51 (t, 2H; *p*-H of second-layer dendron C_6H_3), 6.65 (d, 4H; *o*-H of second- layer dendron C_6H_3), 6.76 (t, 1H; *p*-H of first-layer dendron C_6H_3), 7.29 (d, 2H; *o*-H of first-layer dendron C_6H_3), 7.45 and 8.02 (d, 16H; dendron C_6H_4).

2b (Figure 2)**.** Zn powder (1 g) was added to a THF/AcOH (1:1) solution (8 mL) of **2d** (0.65 mmol), and the resulting suspension was vigorously stirred at 25 °C for 20 min. Then, insoluble fractions were filtered off from the reaction mixture, and the filtrate was poured into water (50 mL) and extracted three times with ethyl acetate (50 mL). The combined extract was dried over anhydrous $MgSO_4$, and residue after evaporation to dryness was chromatographed on silica gel with CH_2-

10.1021/ma034221b CCC: $25.00
Published on Web 10/02/2003

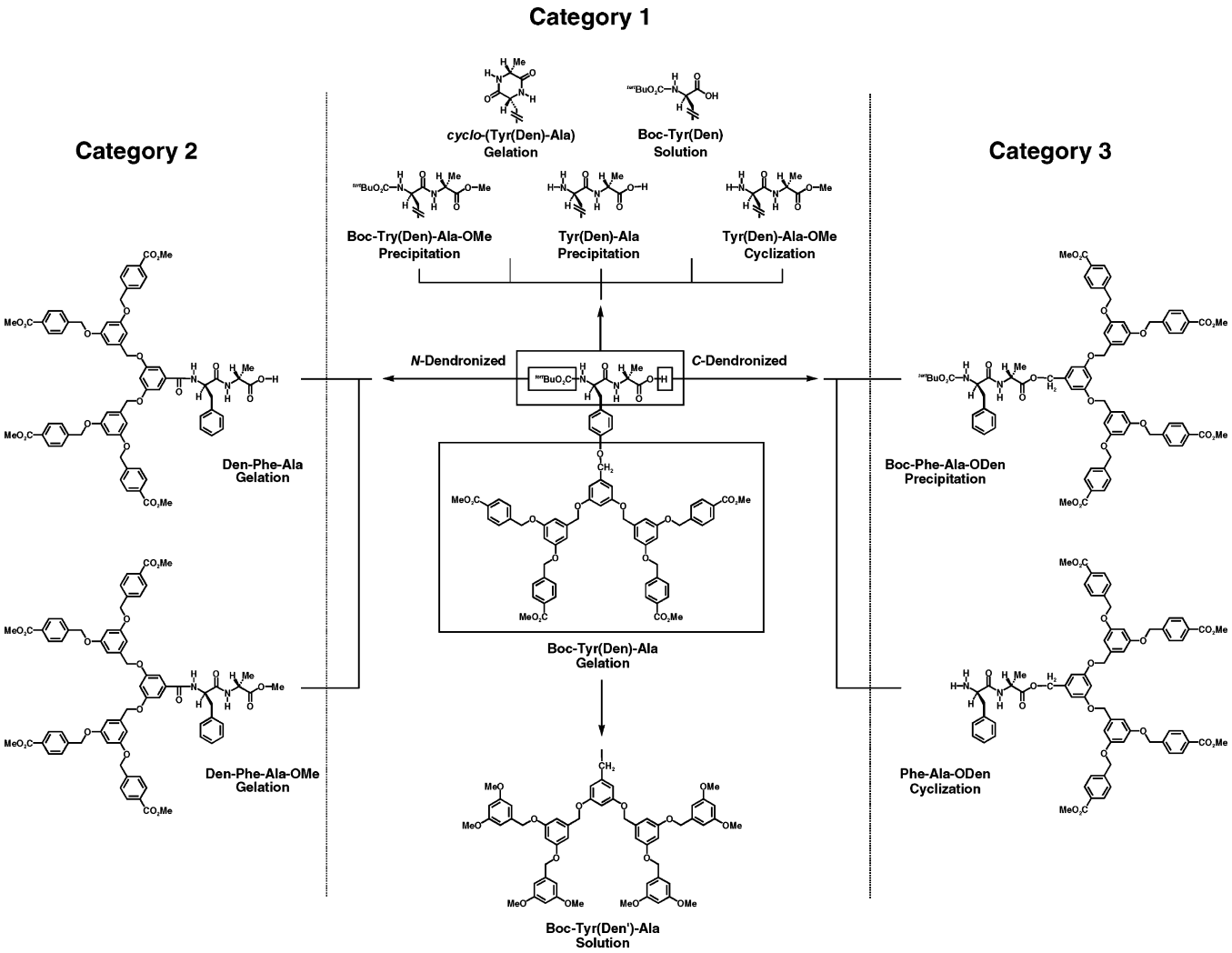

Figure 1. Schematic structures of peptide-core dendritic macromolecules and their gelation activity in MeCN.

Cl_2/EtOH (95/5) as eluent, where the second fraction was collected and freeze-dried from benzene to give **2b** (0.33 mmol) as a white solid in 50% yield. MALDI−TOF-MS for $C_{57}H_{50}O_{16}$ *m*/*z*: calcd, 1013 [M + Na^+]; found, 1012. ^{1}H NMR ($CDCl_3$): δ 3.89 (s, 12H; dendron CO_2CH_3), 4.99 and 5.07 (s, 12H; OCH_2-Ar), 6.52 (t, 2H; *p*-H of second-layer dendron C_6H_3), 6.64 (d, 4H; *o*-H of second-layer dendron C_6H_3), 6.75 (t, 1H; *p*-H of first-layer dendron C_6H_3), 7.26 (d, 2H; *o*-H of first-layer dendron C_6H_3), 7.45 and 8.01 (d, 16H; dendron C_6H_4).

Tyr(Den)-Ala. To a CH_2Cl_2 solution (5 mL) of Boc-Tyr(Den)-Ala (0.076 mmol) was added CF_3CO_2H (0.01 mol), and the mixture was vigorously stirred at 25 °C for 2 h. The reaction mixture was then evaporated to dryness, and the residue, poured into water, was extracted three times with ethyl acetate (50 mL). The combined extract was evaporated to dryness, and the residue was freeze-dried from benzene to give Tyr(Den)-Ala as a white solid in a quantitative yield. MALDI−TOF-MS for $C_{69}H_{66}N_2O_{18}$ *m*/*z*: calcd, 1234 [M + Na^+]; found, 1233. ^{1}H NMR ($CDCl_3$): δ 1.15 (d, 3H; CH_3 of Ala), 2.56 and 2.85 (m, 2H; CH_2Ar of Tyr), 3.67 (s, 12H; dendron CO_2CH_3), 3.95 (m, 1H; CH of Tyr), 4.32 (m, 1H; CH of Ala), 4.72, 4.83, and 4.87 (s, 14H; OCH_2Ar), 6.25, 6.30, and 6.42 (m, 9H; *o*, *p*-H of dendron C_6H_3), 6.52 and 6.82 (d, 4H; C_6H_4 of Tyr), 7.26 and 7.78 (d, 16H; dendron C_6H_4).

Tyr(Den)-Ala-OMe. To a CH_2Cl_2 solution (2 mL) of Boc-Tyr(Den)-Ala-OMe (0.176 mmol) was added CF_3CO_2H (0.02 mol), and the mixture was vigorously stirred at 25 °C for 1 h. Then, the reaction mixture was treated in a manner similar to that for the preparation of Tyr(Den)-Ala to give Tyr(Den)-Ala-OMe as a white solid in a quantitative yield. MALDI−TOF-MS for $C_{70}H_{68}N_2O_{18}$ *m*/*z*: calcd, 1225 [M^+]; found, 1225. ^{1}H NMR ($CDCl_3$): δ 1.32 (d, 3H; CH_3 of Ala), 2.78 (m, 2H; CH_2-Ar of Tyr), 3.63 (s, 3H; CO_2CH_3 of *C*-terminal) 3.87 (s, 12H; dendron CO_2CH_3), 4.27 (m, 1H; CH of Tyr), 4.37 (m, 1H; CH of Ala), 4.84, 4.88, and 5.01 (s, 14H; OCH_2Ar), 6.45 and 6.48 (m, 3H; *o*, *p*-H of first-layer dendron C_6H_3), 6.57 and 6.60 (m, 6H; *o*, *p*-H of second-layer dendron C_6H_3), 6.83 and 7.17 (d, 4H; C_6H_4 of Tyr), 7.41 and 7.98 (d, 8H; dendron C_6H_4).

Cyclo-(Tyr(Den)-Ala). A THF (1 mL) solution of Tyr(Den)-Ala-OMe (0.08 mmol) was stirred at 70 °C for 30 min. The reaction mixture was then evaporated to dryness, and the residue was subjected to preparative HPLC with $CHCl_3$/EtOH (11:1) as eluent to give cyclo-(Tyr(Den)-Ala) (0.05 mmol) as a white solid in 63% yield. MALDI−TOF-MS for $C_{69}H_{64}N_2O_{17}$ *m*/*z*: calcd, 1193 [M^+]; found, 1193. ^{1}H NMR (DMSO-d_6): δ 0.45 (d, 3H; CH_3 of Ala), 2.74 and 3.02 (d, 2H; CH_2Ar of Tyr), 3.82 (s, 12H; dendron CO_2CH_3), 4.10 (m, 2H; CH of Ala and Tyr), 4.98 and 5.17 (s, 6H; OCH_2Ar), 6.53, 6.61, and 6.69 (m, 9H; *o*, *p*-H of dendron C_6H_3), 6.88 and 7.02 (d, 4H; C_6H_4 of Tyr), 7.53 and 7.94 (d, 16H; dendron C_6H_4).

Boc-Tyr(Den). A *N*-methylpyrolidone (NMP) solution (15 mL) of a mixture of **2a** (0.29 mmol; Figure 2), Boc-Tyr (0.32 mmol), and K_2CO_3 (1.28 mmol) was stirred under Ar at 70 °C for 3 h. The reaction mixture was treated in a manner similar to that for the preparation of Boc-Tyr(Den)-Ala-OMe to give Boc-Tyr(Den) as a white solid in 98% yield. MALDI−TOF-MS for $C_{71}H_{69}NO_{19}$ *m*/*z*: calcd, 1263 [M + Na^+]; found, 1263. ^{1}H NMR ($CDCl_3$): δ 1.23 (s, 9H; *tert*-Bu), 2.93 (m, 2H; CH_2Ar of Tyr), 3.76 (s, 12H; dendron CO_2CH_3), 4.30 (m, 1H; CH of Tyr), 4.81, 4.88, and 4.94 (s, 14H; OCH_2Ar), 5.12 (d, 1H; NH), 6.37 and 6.52 (m, 9H; *o*, *p*-H of dendron C_6H_3), 6.55 and 6.69 (d, 4H; C_6H_4 of Tyr), 7.32 and 7.86 (d, 16H; dendron C_6H_4).

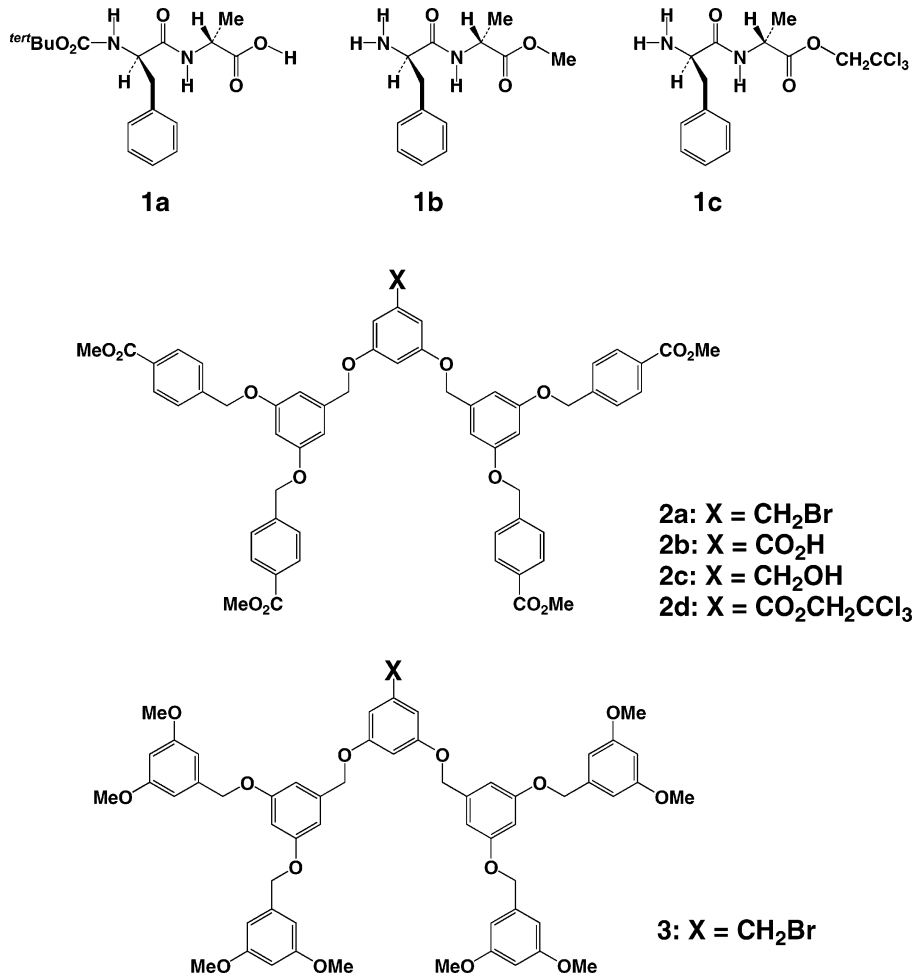

Figure 2. Schematic structures of synthetic precursors for peptide-core dendritic macromolecules.

Boc-(D)-Tyr(Den)-(D)-Ala. A DMF solution (10 mL) of a mixture of **2a** (0.5 mmol; Figure 2) and Boc-(D)-Tyr-(D)-Ala (0.5 mmol), containing K_2CO_3 (2.0 mmol), was stirred under Ar at 70 °C for 3 h. The reaction mixture was treated in a manner similar to that for the preparation of Boc-Tyr(Den)-Ala-OMe to give Boc-(D)-Tyr(Den)-(D)-Ala (0.38 mmol) as a white solid in 76% yield. MALDI−TOF-MS for $C_{74}H_{74}N_2O_{20}$ *m*/*z*: calcd, 1333 [M + Na^+]; found, 1334. ^{1}H NMR ($CDCl_3$): δ 1.28 (d, 3H; C-Me), 1.38 (s, 9H; *tert*-Bu), 2.93 (m, 2H; C−CH_2− Ar of Tyr), 3.89 (s, 12H; CO_2Me), 4.26 (m, 1H; C−H of Ala), 4.48 (t, 1H; C−H of Tyr), 4.93 (s, 4H; second-layer ArO−CH_2− Ar), 4.99 (s, 2H; first-layer ArO−CH_2−Ar), 5.06 (s, 8H; third-layer ArO−CH_2−Ar), 5.46 (d, 1H; N−H of Tyr), 6.26 (d, 1H; N−H of Ala), 6.49−6.66 (m, 9H; *o*, *p*-H of C_6H_3), 6.69 and 6.97 (d, 4H; C_6H_4 of Tyr), 7.43 and 8.00 (d, 8H; dendron C_6H_4).

Boc-Tyr(Den′)-Ala. A *N*,*N*-dimethylformamide (DMF) solution (15 mL) of a mixture of **3** (0.32 mmol; Figure 2), Boc-Tyr-Ala (0.32 mmol), and K_2CO_3 (0.8 mmol) was stirred under Ar at 70 °C for 3 h. The reaction mixture was treated in a manner similar to that for the preparation of Boc-Tyr(Den)-Ala-OMe to give Boc-Tyr(Den′)-Ala (0.20 mmol) as a white solid in 62% yield. MALDI−TOF-MS for $C_{74}H_{82}N_2O_{20}$ *m*/*z*: calcd, 1359 [M + K^+]; found, 1359. ^{1}H NMR ($CDCl_3$): δ 1.29 (d, 3H; CH_3 of Ala), 1.35 (s, 9H; *tert*-Bu), 2.91 (m, 2H; CH_2Ar of Tyr), 3.73 (s, 24H; dendron OCH_3), 4.25 (m, 1H; CH of Tyr), 4.50 (t, 1H; CH of Ala), 4.91 (sh), 4.92, and 5.03 (s, 14H; OCH_2Ar), 6.36, 6.52, and 6.62 (m, 21H; *o*, *p*-H of dendron C_6H_3), 6.68 and 6.96 (d, 4H; C_6H_4 of Tyr).

Den-Phe-Ala-OTce. A **1c**·HCl salt (1.54 mmol; Figure 2) was added to a DMF solution (10 mL) of **2b** (1.54 mmol; Figure 2), and the mixture was neutralized with 2,4,6-collidine (1.82 mmol). Benzotriazol-1-ol (HOBt; 1.54 mmol) and *N*,*N*′-dicyclohexylcarbodiimide (DCC; 1.54 mmol) were then added to the above solution, and the mixture was vigorously stirred under Ar at 0 °C for 3 h and then 25 °C for 20 h. Insoluble fractions were filtered off from the reaction mixture, and the filtrate was subjected to reprecipitation from MeOH. The precipitate was collected and chromatographed on silica gel with CH_2Cl_2 as eluent, where the first fraction was collected and freeze-dried from benzene, to give Den-Phe-Ala-OTce (0.78 mmol) as a white solid in 51% yield. MALDI−TOF-MS for $C_{71}H_{65}Cl_3N_2O_{18}$ *m*/*z*: calcd, 1342 [M + H^+]; found, 1341. ^{1}H NMR (DMSO-d_6): δ 1.41 (d, 3H; CH_3 of Ala), 2.96 and 3.09 (m, 2H; CH_2Ar of Phe), 3.83 (s, 12H; dendron CO_2CH_3), 4.44 (m, 1H; CH of Phe), 4.74 (m, 1H; CH of Ala), 4.91 (q, 2H; OCH_2-CCl_3), 5.03 and 5.17 (s, 12H; OCH_2Ar), 6.64 and 6.71 (m, 6H; *o*, *p*-H of second-layer dendron C_6H_3) 6.75 and 7.03 (m, 3H; *o*, *p*-H of first-layer dendron C_6H_3), 7.20 (m, 5H; C_6H_5 of Phe), 7.54 and 7.94 (d, 16H; dendron C_6H_4).

Den-Phe-Ala. To a THF/AcOH (1:1) solution (100 mL) of Den-Phe-Ala-OTce (0.15 mmol) was added Zn powder (400 mg), and the resulting suspension was treated in a manner similar to that for the preparation of **2b** (Figure 2) to give Den-Phe-Ala (0.10 mmol) as a white solid in 66% yield. MALDI−TOF-MS for $C_{69}H_{64}N_2O_{18}$ *m*/*z*: calcd, 1232 [M + Na^+]; found, 1231. ^{1}H NMR (DMSO-d_6): δ 1.35 (d, 3H; CH_3 of Ala), 3.17 (m, 2H; CH_2Ar of Phe), 3.89 (s, 12H; dendron CO_2CH_3), 4.19 (m, 1H; C−H of Phe), 4.47 (m, 1H; CH of Ala), 4.92 and 5.06 (s, 12H; OCH_2Ar), 6.51, 6.59, and 6.84 (m, 9H; *o*, *p*-H of dendron C_6H_3), 7.24 (m, 5H; C_6H_5 of Phe), 7.43 and 8.00 (d, 8H; dendron C_6H_4).

Den-Phe-Ala-OMe. A **1b**·HCl salt (0.32 mmol; Figure 2) was added to a DMF solution (2 mL) of **2b** (0.18 mmol; Figure 2), and the mixture was neutralized with 2,4,6-collidine (0.32 mmol). HOBt (0.32 mmol) and DCC (0.32 mmol) were then added to the above solution, and the reaction mixture was treated in a manner similar to that for the preparation of Den-Phe-Ala-OTce to give Den-Phe-Ala-OMe (0.09 mmol) as a white solid in 49% yield. MALDI−TOF-MS for $C_{70}H_{66}N_2O_{18}$ *m*/*z*:

calcd, 1224 [M + H^+]; found, 1224. ^{1}H NMR ($CDCl_3$): δ 1.32 (d, 3H; CH_3 of Ala), 3.17 (m, 2H; CH_2Ar of Phe), 3.70 (s, 3H; CO_2CH_3 of Ala), 3.90 (s, 6H; dendron CO_2CH_3), 4.46 (m, 1H; CH of Phe), 4.80 (m, 1H; CH of Ala), 4.95 and 5.08 (s, 12H; OCH_2Ar), 6.22 and 6.82 (d, H; NH of Phe), 6.53, 6.63, and 6.89 (m, 9H; *o*, *p*-H of dendron C_6H_3), 5.56 (1H; NH of Ala), 7.26 (m, 5H; C_6H_5 of Phe), 7.45 and 8.00 (d, 16H; dendron C_6H_4).

Boc-Phe-Ala-ODen. To a THF (10 mL) suspension of a mixture of **1a** (0.51 mmol; Figure 2), *N*,*N*-dimethyl-4-aminopyridine (DMAP; 0.62 mmol), and **2b** (0.51 mmol; Figure 2) was added DCC (0.62 mmol), and the resulting mixture was stirred under Ar at 0 °C for 3 h and then at 25 °C for 20 h. Insoluble fractions were filtered off from the reaction mixture, the filtrate was evaporated to dryness, and the residue was chromatographed on silica gel with CH_2Cl_2 as eluent, where the first fraction was collected and freeze-dried from benzene to give Boc-Phe-Ala-ODen (0.29 mmol) as a white solid in 57% yield. MALDI−TOF-MS for $C_{74}H_{74}N_2O_{19}$ *m*/*z*: calcd, 1318 [M + Na^+]; found, 1318. ^{1}H NMR ($CDCl_3$): δ 1.32 (d, 3H; CH_3 of Ala), 1.36 (s, 9H; *tert*-Bu), 3.02 (d, 2H; CH_2Ar of Phe), 3.90 (s, 12H; dendron CO_2CH_3), 4.32 (m, 1H; CH of Phe), 4.54 (m, 1H; CH of Ala), 4.94, 5.04, and 5.07 (s, 14H; OCH_2Ar), 6.29 (1H; NH of Ala), 6.50 and 6.64 (m, 6H; *o*, *p*-H of second-layer dendron C_6H_3), 6.69 and 6.97 (d, 3H; C_6H_3 of first-layer dendron C_6H_3), 7.18 (m, 5H; C_6H_5 of Phe), 7.45 and 8.01 (d, 16H; dendron C_6H_4).

Phe-Ala-ODen. To a CH_2Cl_2 solution (2 mL) of Boc-Phe-Ala-ODen (0.077 mmol) was added HCO_2H (4 mL), and the resulting mixture was vigorously stirred at 25 °C for 18 h. The reaction mixture was then evaporated to dryness, and the residue was freeze-dried from benzene to give Phe-Ala-ODen as white solid in a quantitative yield. MALDI−TOF-MS for $C_{69}H_{66}N_2O_{17}$ *m*/*z*: calcd, 1195 [M^+]; found, 1194. ^{1}H NMR ($CDCl_3$): δ 1.37 (d, 3H; CH_3 of Ala), 2.68 and 3.20 (m, 2H; CH_2-Ar of Phe), 3.61 (m, 1H; CH of Phe), 3.90 (s, 12H; dendron CO_2CH_3), 4.62 (m, 1H; CH of Ala), 4.94 and 5.05 (s, 14H; OCH_2-Ar), 6.52 and 6.63 (m, 9H; *o*, *p*-H of dendron C_6H_3), 7.22 (m, 5H; C_6H_5 of Phe), 7.45 and 8.01 (d, 8H; C_6H_4 of dendron).

Procedures: Gelation Experiments. Typically, a suspension of Boc-Tyr(Den)-Ala (5 mg) in MeCN (3 mL) was heated in a screw-capped glass bottle until it became clear. The resulting solution was sonicated for 1 min and then allowed to stand at 20 °C, whereupon it became immobile. The resulting gel was placed on a glass plate overnight under air at 20 °C and then vacuum-pumped in a desiccator to give a dry gel. For determining the critical concentration for gelation, varying amounts of Boc-Tyr(Den)-Ala were employed (Figure 3A−D), and the systems obtain after the above treatment were centrifuged. When the concentration of Boc-Tyr(Den)-Ala was lower than the critical concentration for gelation, excess MeCN was separated from a frozen (gel) phase upon centrifugation. On increment of the concentration of Boc-Tyr(Den)-Ala, the amount of MeCN separated became smaller, and finally no phase separation was observed when the system reached the critical concentration for gelation.

Measurements: Instruments. Preparative recycling HPLC was carried out on a JAI model LC-918 equipped with a JAIGEL-SIL SHO43-10 column. ^{1}H NMR spectra were measured in $CDCl_3$ or DMSO-d_6 at 21 °C on a JEOL model GSX-270 spectrometer operating at 270 MHz, where the chemical shifts were determined with respect to $CHCl_3$ (δ 7.28 ppm) or CD_3SOCD_2H (δ 2.49 ppm) as an internal reference. Matrix-assisted laser desorption ionization time-of-flight mass spectrometry (MALDI−TOF-MS) was performed on a Bruker model ProteinTof mass spectrometer using 9-nitroanthracene (9NA) or indole acetic acid (IAA) as a matrix. Cross-polarized microscopy was carried out on a Nikon model Optiphot microscope coupled with a Mettler model FP82HT hot stage. Differential scanning calorimetry (DSC) was performed on a Mettler model DSC 30.

Field Emission Scanning Electron Microscopy (FE-SEM). Dry gels on a glass plate were spattered with Pt under an electric current of 15 mA at 10 Pa for 5−10 s. Electron micrographs were recorded on a Hitachi model S-900 operating at 5 kV.

X-ray Diffraction (XRD) Analysis. Glass plates with dry gels were fixed on a sample holder and subjected to XRD analysis at room temperature on a Rigaku RINT2000 diffractometer operating with a line-focused Cu Kα radiation beam.

Circular Dichroism (CD) and Linear Dichroism (LD) Spectroscopy. CD spectra were recorded on a JASCO model J-720 spectropolarimeter using a quartz cell of 0.1 or 1 mm path length depending on the substrate concentration. Linear dichroism (LD) spectra were recorded on a JASCO model J-820 spectropolarimeter at 20 °C.

Infrared (IR) and Variable-Temperature IR (VT-IR) Spectroscopy. IR spectra were recorded on a JASCO model FT/IR 610 spectrometer using CaF_2 windows and corrected for the solvents. Variable-temperature IR (VT-IR) spectra were recorded on a JASCO model MFT 2000 spectrometer coupled with a Mettler model FP82HT hot stage.

Results and Discussion

As reported previously, a N-protected tyrosinylalanine with an ester-terminated poly(benzyl ether) dendritic side group, Boc-Tyr(Den)-Ala (Figure 1), efficiently forms a transparent physical gel in MeCN, where nearly 20 000 solvent molecules are frozen by one molecule of Boc-Tyr(Den)-Ala.[8] A detailed investigation has shown that inter-dendrimer interactions serve cooperatively with hydrogen-bonding interactions at the focal core to stabilize the self-organized fibrous structure.

To investigate the structure−property relationship for physical gelation, 10 different peptide-core dendritic macromolecules bearing a [G2] poly(benzyl ether) dendritic wedge (Den) were newly synthesized (Figure 1), and their potentials as macromolecular organic gelators were investigated. These dendritic macromolecules are classified into three categories, according to the topology of the dendritic wedge. The first category includes Boc-Tyr(Den)-Ala-OMe, Tyr(Den)-Ala, Tyr(Den)-Ala-OMe, cyclo-(Tyr(Den)-Ala), and Boc-Tyr(Den) (category 1); each bears an ester-terminated dendritic side chain, similar to Boc-Tyr(Den)-Ala. We also synthesized Boc-Tyr(Den′)-Ala, whose dendritic wedge has methoxy groups, in place of ester functionalities, on the exterior surface. The dendritic macromolecules in category 1 should allow us to investigate possible structural effects of the core module and the surface group on the gelation. Category 2 includes Den-Phe-Ala and Den-Phe-Ala-OMe, which possess a dendritic wedge at the N-terminal (N-dendronized). On the other hand, category 3 includes Boc-Phe-Ala-ODen and Phe-Ala-ODen, which bear a dendritic wedge at the C-terminal (C-dendronized). The dendritic macromolecules in the latter two categories should allow us to investigate topological effects of the dendritic wedge on the gelation.

(A) Gelation Properties. Gelation properties of the newly synthesized dendritic macromolecules are summarized in Table 1, together with those of previously studied Boc-Tyr(Den)-Ala as a reference.[8] When a clear solution, obtained by heating an MeCN suspension of cyclo-(Tyr(Den)-Ala), was sonicated for 1 min and allowed to stand overnight at 20 °C, it gradually became viscous and finally turned immobile. In contrast with the case of Boc-Tyr(Den)-Ala, which forms a transparent gel (Figure 3C,D), the gel of cyclo-(Tyr(Den)-Ala) was slightly opaque (Figure 3E). The critical concentration for gelation with cyclo-(Tyr(Den)-Ala) was found to be 1.4 mM, which is comparable to that of Boc-Tyr(Den)-Ala (1.0 mM). On the other hand, a hot MeCN solution of Boc-Tyr(Den)-Ala-OMe, a methyl ester version of Boc-Tyr(Den)-Ala, afforded, on cooling to 20 °C, a birefringent precipitate without gelation. A dipeptide-core

Table 1. Gelation Activities of Peptide-Core Dendritic Macromolecules in MeCN at 20 °C

peptide-core dendritic macromolecules	appearance	critical concn for gelation [mM]	T_m [°C]
category 1: side-chain dendronized			
Boc-Tyr(Den)-Ala	transparent gel	1.0	112
Boc-Tyr(Den)-Ala-OMe	precipitation		
Tyr(Den)-Ala	precipitation		
Tyr(Den)-Ala-OMe[a]			
Boc-Tyr(Den′)-Ala	homogeneous solution		
cyclo-(Tyr(Den)-Ala)	slightly opaque gel	1.4	n.d.
Boc-Tyr(Den)	homogeneous solution		
category 2: N-dendronized			
Den-Phe-Ala	opaque gel	2.2	209
Den-Phe-Ala-OMe	opaque gel	1.4	214
category 3: C-dendronized			
Boc-Phe-Ala-ODen	precipitation		
Phe-Ala-ODen[a]			

[a] Cyclization of the dipeptide core concomitantly took place.

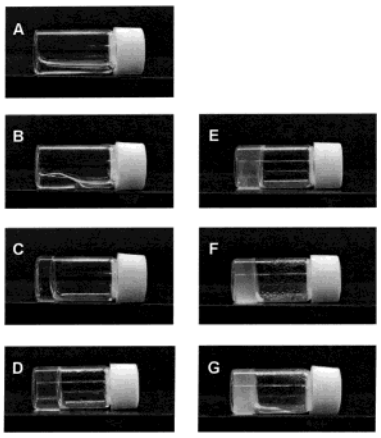

Figure 3. Pictures of MeCN suspensions of Boc-Tyr(Den)-Ala at different concentrations: (A) 0.4, (B) 0.8, (C) 1.5, and (D) 2.7 mM and those of (E) cyclo-(Tyr(den)-Ala), (F) Den-Phe-Ala, and (G) Den-Phe-Ala-OMe at 2.7 mM, when allowed to stand for 12 h after heated for 1 min and then sonicated for 1 min.

dendritic macromolecule with an unprotected N-terminal such as Tyr(Den)-Ala-OMe, upon heating in MeCN, easily underwent intramolecular cyclization to give gel-forming cyclo-(Tyr(Den)-Ala) with the release of MeOH. A zwitterionic dipeptide-core dendritic macromolecule such as Tyr(Den)-Ala was hardly soluble in MeCN even upon heating. In sharp contrast, Boc-Tyr(Den), a monopeptide version of Boc-Tyr(Den)-Ala, was highly soluble in MeCN and did not form a gel even at a high concentration such as 17.5 mM.

The dendritic macromolecules in categories 2 and 3 showed contrasting gelation properties to one another. N-dendronized dipeptides (category 2) such as Den-Phe-Ala and Den-Phe-Ala-OMe efficiently formed physical gels in MeCN with the critical concentrations for gelation of 2.2 and 1.4 mM, respectively. The gels were highly opaque (Figure 3F,G), different from those with side-chain-dendronized dipeptides Boc-Tyr(Den)-Ala and cyclo-(Tyr(Den)-Ala). In sharp contrast with the side-chain and N-dendronized dipeptides (categories 1 and 2), C-dendronized dipeptides (category 3) such as Boc-Phe-Ala-ODen and Phe-Ala-ODen hardly underwent gelation, regardless of whether the N-terminal was protected or free: Boc-Phe-Ala-ODen was sparingly soluble even in hot MeCN. On the other hand, similar to Tyr(Den)-Ala-OMe, Phe-Ala-ODen, upon heating, readily underwent intramolecular cyclization to generate dendritic alcohol **2c** (Figure 2) and highly insoluble cyclic dipeptide cyclo-(Phe-Ala). We also found that the

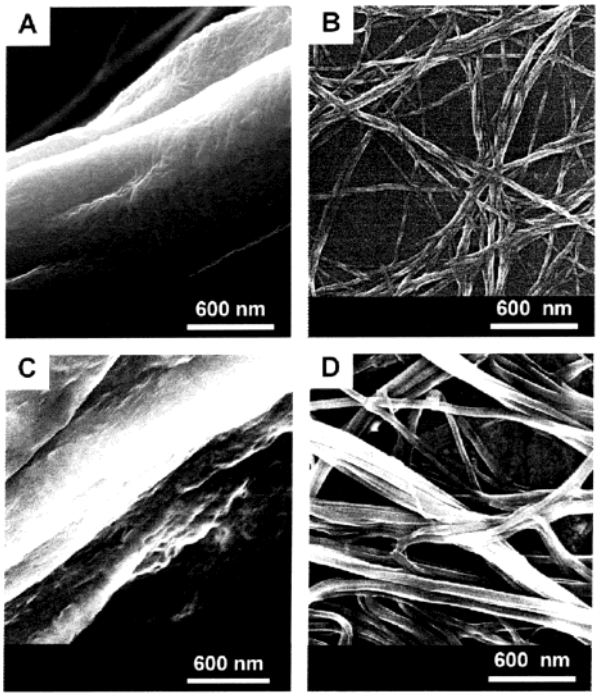

Figure 4. Field emission scanning electron micrographs (FE-SEM) of dry gels: (A) Boc-Tyr(Den)-Ala, (B) cyclo-(Tyr(Den)-Ala), (C) Den-Phe-Ala, and (D) Den-Phe-Ala-OMe.

surface group of the dendritic wedge plays a significant role in gelation. For example, Boc-Tyr(Den′)-Ala, which bears methyl ether groups on the surface of the dendritic wedge, was highly soluble in MeCN and did not cause gelation.

As described above, among the 11 peptide-core dendritic macromolecules (Figure 1), cyclo-(Tyr(Den)-Ala), Den-Phe-Ala, and Den-Phe-Ala-OMe, as well as previously studied Boc-Tyr(Den)-Ala, are capable of forming physical gels in MeCN. We noted that the gel with Den-Phe-Ala-OMe is more brittle than the others. All the gels thus formed became mobile to flow upon heating, while the resulting hot melts gradually turned immobile when allowed to stand at room temperature (thixotropy).

When the gels were dried, fibrous assemblies resulted. Field emission scanning electron micrographs (FE-SEM) of the dry gels with Boc-Tyr(Den)-Ala (Figure 4A) and Den-Phe-Ala (Figure 4C) both displayed fibers with a diameter of 0.5−1.0 μm, which consist of a great number of much thinner elementary fibrils with a diameter of approximately 20 nm. On the other hand, FE-SEM

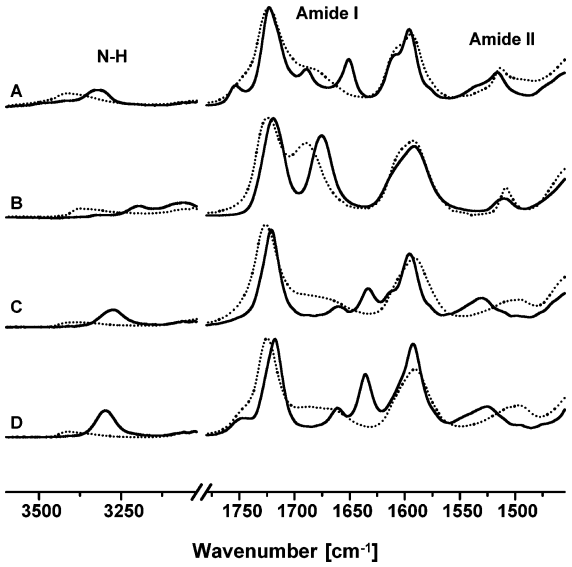

Figure 5. Infrared spectra of dry gels before (solid curves) and after heated above T_m (broken curves).

micrographs of the dry gels with cyclo-(Tyr(Den)-Ala) (Figure 4B) and Den-Phe-Ala-OMe (Figure 4D) showed tape-like bundles of 30−60 nm wide self-assembled nanoribbons.

(B) Spectral Characteristics of Gels. Infrared spectra of the physical gels, formed in MeCN with Boc-Tyr(Den)-Ala, cyclo-(Tyr(Den)-Ala), Den-Phe-Ala, and Den-Phe-Ala-OMe, all showed characteristic vibrational bands due to hydrogen-bonding interactions in the N−H (3400−3200 cm^{-1}), amide I (1685−1625 cm^{-1}), and amide II (1560−1520 cm^{-1}; except for cyclo-(Tyr(Den)-Ala)) regions.[12] Furthermore, even after dried, all the gels retained their spectral characteristics (solid curves, Figure 5). For example, the dry gel with Boc-Tyr(Den)-Ala[8] displays a broad N−H stretching vibrational band centered at 3320 cm^{-1}, while amide I stretching bands at 1650 and 1685 cm^{-1} and an amide II band at 1534 cm^{-1} (Figure 5A). On the other hand, a homogeneous $CHCl_3$ solution of Boc-Tyr(Den)-Ala, as a non-hydrogen-bonded reference, displayed a N−H stretching vibrational band at 3420 cm^{-1} ($\Delta\nu = +200$ cm^{-1}), while amide I and II bands at 1675 (sh, 1700) ($\Delta\nu = +25$ cm^{-1}) and 1498 cm^{-1} ($\Delta\nu = -36$ cm^{-1}), respectively. These spectral characteristics, together with the shape of the amide I band, indicate that the dipeptide functionality of Boc-Tyr(Den)-Ala in the dry gel most likely forms an anti-parallel β-sheet structure.[12] Interestingly, the C-terminal carbonyl group of the carboxylic acid functionality exhibited a vibrational band at 1752 cm^{-1}, typical of non-hydrogen-bonded $-CO_2H$ (Figure 5A). Thus, the carboxylic acid moiety of Boc-Tyr(Den)-Ala is not involved in the hydrogen-bonding interactions for the formation of the anti-parallel β-sheet structure. The same was true for the dry gel with Den-Phe-Ala-OMe (Figure 5D), where the $-CO_2Me$ group ($\nu_{C=O}$ = 1745 cm^{-1}) is not incorporated into the hydrogen-bonded dipeptide network ($\nu_{C=O}$ = 1635 [sh, 1660] and 1525 cm^{-1} for amide I and II bands, respectively). Judging from the spectral pattern of the amide region, the dipeptide functionality of Den-Phe-Ala-OMe in the self-organized structure likely forms a syn-parallel β-sheet structure.[12]

The dry gel with Den-Phe-Ala, bearing a carboxylic acid functionality at the C-terminal, showed virtually

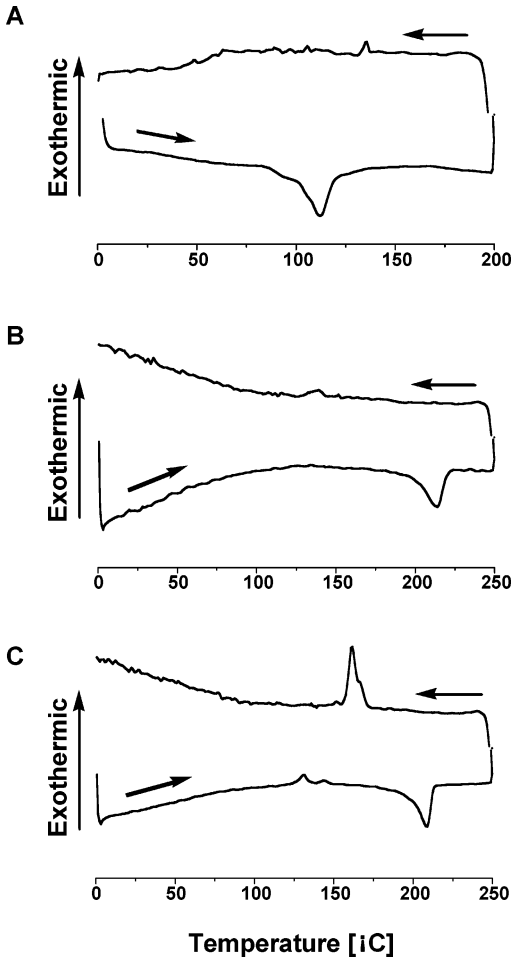

Figure 6. Differential scanning calorimetry (DSC) profiles of dry gels: (A) Boc-Tyr(Den)-Ala, (B) Den-Phe-Ala, and (C) Den-Phe-Ala-OMe.

the same infrared spectral profile (Figure 5C) as that with Den-Phe-Ala-OMe, adopting a syn-parallel β-sheet structure (Figure 5D). However, the absence of any peaks at 1760−1740 cm^{-1} indicates a shift of the vibrational band of the terminal $-CO_2H$ moiety toward a low-frequency region, as the result of hydrogen-bonding interactions.[12] On the other hand, the spectral pattern of the dry gel with cyclo-(Tyr(Den)-Ala) (Figure 5B) was essentially different from those of the others. Taking into account the ribbonlike fibrous morphology of the dry gel (Figure 4B) and also the general trend of the hydrogen-bonding characteristics of cyclic dipeptide derivatives,[13] the spectral profile observed for the dry gel with cyclo-(Tyr(Den)-Ala) may indicate the presence of linear hydrogen-bonded arrays of the dipeptide functionalities.

(C) Thermal Properties of Dry Gels. Upon heating from 0 °C at a rate of 10 °C min^{-1}, the dry gel with Boc-Tyr(Den)-Ala displayed, in differential scanning calorimetry (DSC, Figure 6A), a broad endothermic peak at 112 °C (40.3 kJ mol^{-1}), which corresponds to the melting temperature (T_m) of the self-assembled structure, as observed by cross-polarized optical microscopy. When the heating process from 100 to 128 °C was traced by infrared spectroscopy, the dry gel obviously lost all the structural characteristics associated with the hydrogen-bonding interactions among the dipeptide focal cores (Figure 7). As expected, the observed T_m was much higher than that of the corresponding dipeptide-free dendritic alcohol (**2c**, T_m = 60 °C). In relation to this

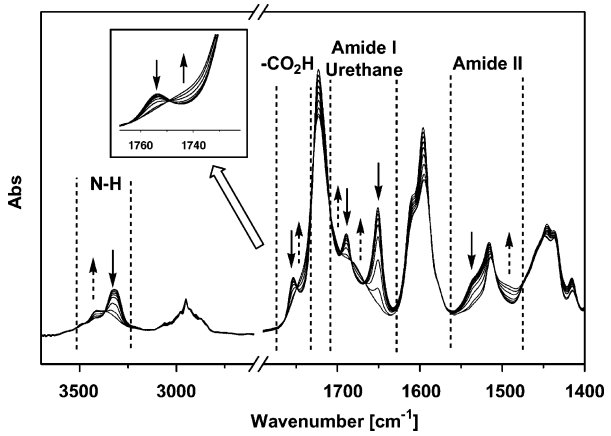

Figure 7. Variable-temperature infrared (VT-IR) spectra of a dry gel with Boc-Tyr(Den)-Ala at 100−128 °C at a heating rate of 10 °C min^{-1}.

observation, the dry gels with N-dendronized dipeptides, Den-Phe-Ala (Figure 6B) and Den-Phe-Ala-OMe (Figure 6C), displayed T_m peaks at 209 (65.0 kJ mol^{-1}) and 214 °C (63.8 kJ mol^{-1}), respectively, which are much higher by 100 °C than that of Boc-Tyr(Den)-Ala. As shown by the broken curves in Figure 5, the infrared spectra of the dry gels, when heated above T_m, all became more like those of dilute solutions, as the result of a thermal breakdown of the intermolecular hydrogen bonds.

Among the three gel-forming dendritic dipeptides Boc-Tyr(Den)-Ala, Den-Phe-Ala, and Den-Phe-Ala-OMe, only the last one with an esterified C-terminal showed a reversible DSC profile. When the dry gel with Den-Phe-Ala-OMe, once melted, was allowed to cool to 0 °C at a rate of 10 °C min^{-1}, an intense exothermic peak appeared at 166 °C (52.8 kJ mol^{-1}) (Figure 6C). In the second heating of the resulting sample at a rate of 10 °C min^{-1}, an endothermic peak again appeared at 212 °C (58.7 kJ mol^{-1}). Accordingly, the dry gel with Den-Phe-Ala-OMe showed a thermally reversible infrared spectral change profile. In sharp contrast, the dry gels with Boc-Tyr(Den)-Ala and Den-Phe-Ala displayed irreversible DSC profiles, where no obvious phase transitions, other than glass transition, were observed in both the first cooling and the second heating processes (Figure 6A,B). Accordingly, when the dry gel with Boc-Tyr(Den)-Ala was heated above T_m, a new vibrational band, assignable to a dimeric form of $-CO_2H$, appeared at 1740 cm^{-1} at the expense of the vibrational band at 1752 cm^{-1} due to the non-hydrogen-bonded $-CO_2H$ functionality (Figure 7). This observation indicates that the dimerization of the carboxylic acid terminal, a thermodynamically favored process, is kinetically prevented by a certain steric regulation in the gel-forming self-organization event.

(D) Structural Aspects of Gels. As shown in Figure 8A, the dry gel with side-chain-dendronized Boc-Tyr-(Den)-Ala displayed two intense X-ray diffractions at d = 56 and 38 Å. Similarly, the dry gel with N-dendronized Den-Phe-Ala-OMe (Figure 8C) showed two major diffractions at d = 48 and 26 Å, in addition to several minor diffractions. In contrast, the dry gel with N-dendronized Den-Phe-Ala displayed a major diffraction at d = 55 Å, together with two broad diffractions (Figure 8B). By taking into consideration the infrared spectral profiles of the dry gels in regard to the relative orientation of the dipeptide cores, we propose, on the basis of the above XRD patterns, possible self-organized

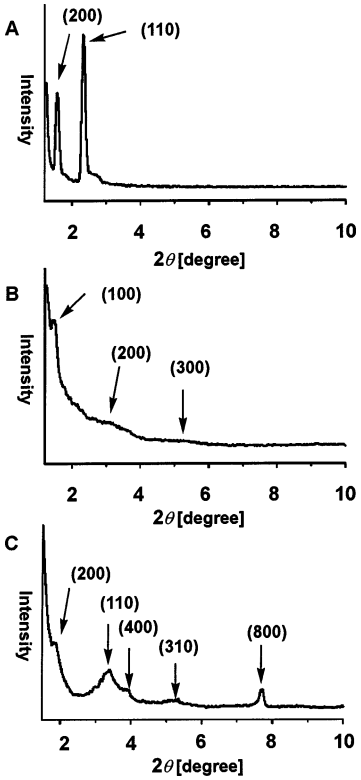

Figure 8. X-ray diffraction (XRD) profiles of dry gels: (A) Boc-Tyr(Den)-Ala, (B) Den-Phe-Ala, and (C) Den-Phe-Ala-OMe.

structures of the dipeptide-core dendritic macromolecules (Figure 9). The schematic structures in Figure 9A (Boc-Tyr(Den)-Ala) and Figure 9C (Den-Phe-Ala-OMe) both involve two facing β-sheet arrays of the dipeptide functionalities, where the former is antiparallel and the latter syn-parallel. In general, rectangular columnar phases display two intense X-ray diffraction peaks in the low-angle region, which can be indexed as (200) and (110) diffractions.[14] Therefore, Boc-Tyr(Den)-Ala and Den-Phe-Ala-OMe most likely form a rectangular columnar phase. The lattice parameters were estimated as a = 112 Å and b = 40 Å for Boc-Tyr-(Den)-Ala, while a = 96 Å and b = 27 Å for Den-Phe-Ala-OMe. In these cases, the C-terminal functionalities, such as $-CO_2H$ of Boc-Tyr(Den)-Ala (Figure 9A) and $-CO_2Me$ of Den-Phe-Ala-OMe (Figure 9C), are embedded in the dendritic frameworks and not eligible for hydrogen-bonding interactions. In contrast with Den-Phe-Ala-OMe, Den-Phe-Ala with an unprotected C-terminal in the dry gel participates in hydrogen-bonding interactions at the $-CO_2H$ moiety (Figure 5C). Furthermore, differently from Boc-Tyr(Den)-Ala (Figures 8A and 9A) and Den-Phe-Ala-OMe (Figures 8C and 9C), Den-Phe-Ala (Figure 8B) showed an XRD pattern characteristic of a lamellar geometry (Figure 9B). The interlamellar separation, as evaluated from the d spacing, was 55 Å, which is consistent with that predicted from a simplified molecular model composed of two molecules of Den-Phe-Ala hydrogen-bonded at the $-CO_2H$ terminal.

When physical gels are transparent, circular dichroism (CD) spectroscopy is informative of molecular packing geometries of chiral gelators. As reported briefly,[8] the transparent gel formed with Boc-(L)-Tyr(Den)-(L)-Ala in MeCN displays strong CD bands at the absorption bands of the dendritic wedge (250−300 nm). We

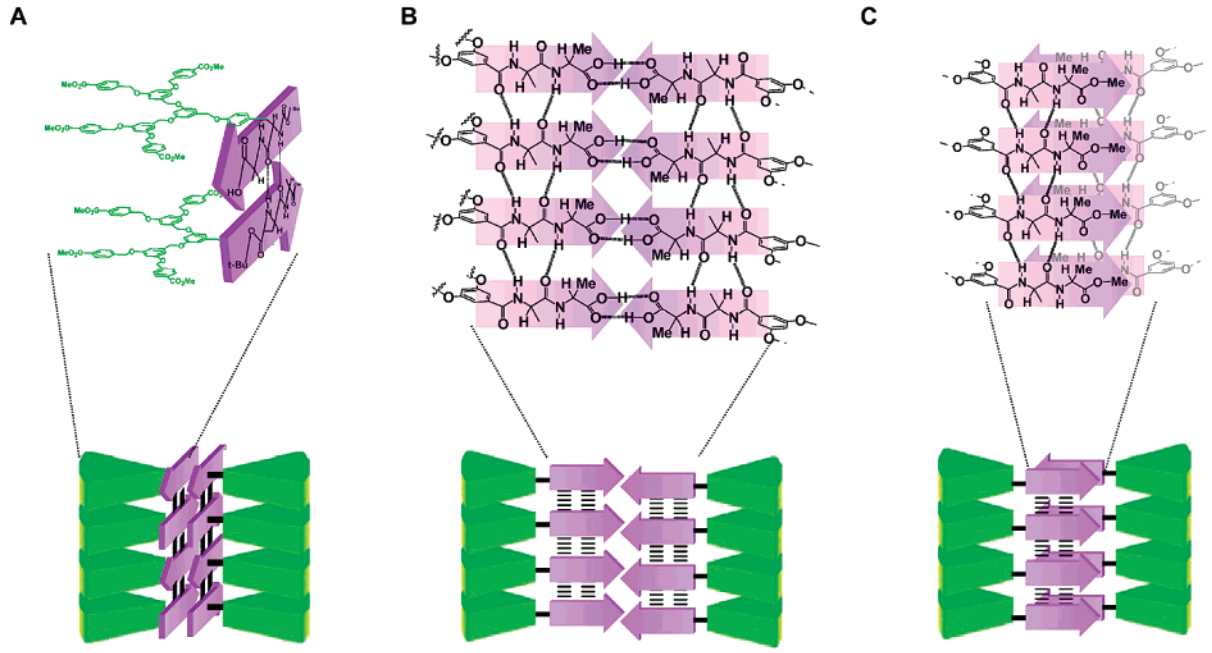

Figure 9. Proposed self-assembled structures of dry gels: (A) Boc-Tyr(Den)-Ala, (B) Den-Phe-Ala, and (C) Den-Phe-Ala-OMe.

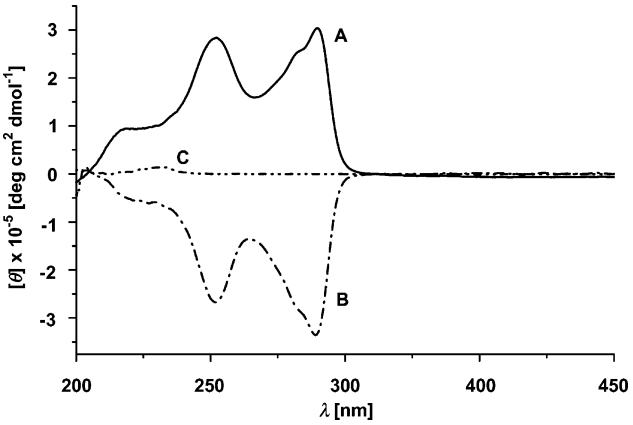

Figure 10. Circular dichroism (CD) spectra at 20 °C of gels prepared in MeCN with Boc-(L)-Tyr(Den)-(L)-Ala (A; 2.2 mM) and Boc-(L)-Tyr(Den)-(L)-Ala (B; 2.2 mM) in a quartz cell of 0.1 mm path length and a nongelled dilute MeCN solution of Boc-(L)-Tyr(Den)-(L)-Ala (C; 0.18 mM) in a quartz cell of 1 mm path length.

newly synthesized Boc-(D)-Tyr(Den)-(D)-Ala and investigated the CD profile of a gel prepared in MeCN at 2.2 mM. As shown in Figure 10, the CD spectrum of the gel was a perfect mirror image of that of Boc-(L)-Tyr-(Den)-(L)-Ala, displaying intense Cotton effects at the absorption bands of the dendritic wedge ($[\theta]_{252} = -2.7 \times 10^5$; $[\theta]_{290} = -3.3 \times 10^5$ deg cm^2 dmol^{-1}). We also confirmed that the observed spectra are hardly contaminated with linear dichroism (LD). On the other hand, a homogeneous dilute MeCN solution of Boc-(L)-Tyr(Den)-(L)-Ala (0.18 mM) exhibited only a negligibly weak CD band at the absorption band of the dipeptide core ($[\theta]_{232} = +1.4 \times 10^4$ deg cm^2 dmol^{-1}), whereas it was CD-silent at 250−300 nm (Figure 10C). Therefore, the intense CD bands observed for the dendritic wedge in Figure 10A,B indicate a helically twisted geometry of the β-sheet arrays composed of hydrogen-bonded Boc-Tyr(Den)-Ala (Figure 9A).[15]

Conclusions

In summary, we investigated the gelation properties of a series of 11 different peptide-core poly(benzyl ether) dendritic macromolecules and obtained the following structural parameters as required for the efficient gelation: (1) dipeptides (including cyclic dipeptides), rather than monopeptides, are favorable as the core units; (2) ester functionalities on the surface of the dendritic wedge play a positive role (inter-dendrimer interaction); (3) side-chain dendronization or N-dendronization of dipeptides is preferred, whereas C-dendronization promotes precipitation; and (4) higher generation numbers of the dendritic wedge are preferred. While introduction of long alkyl chains to hydrogen-bonding modules is a common strategy for the molecular design of organic gelators, some of the above structural parameters such as (2) and (4), in particular, indicate a new insight into the chemistry of physical gels, since dendrimers, in contrast with long hydrocarbons, are usually noncrystalline and possess large hydrodynamic volumes. We believe that dendritic gelators, which can site-specifically accommodate functional groups, would provide a great opportunity for the fabrication of functional supramolecular materials.

References and Notes

(1) Fréchet, J. M. J. *Science* **1994**, *263*, 1710. (b) Tomalia, D. A. *Adv. Mater.* **1994**, *6*, 529. (c) Fischer, M.; Vögtle, F. *Angew. Chem., Int. Ed.* **1999**, *38*, 884.
(2) Tomalia, D. A.; Esfand, R. *Chem. Ind.* **1997**, *11*, 416.
(3) Zimmerman, S. C.; Zeng, F.-W.; Reichert, D. E. C.; Kolotuchin, S. V. *Science* **1996**, *271*, 1095. (b) Suárez, M.; Lehn, J. M.; Zimmerman, S. C.; Skoulios, A.; Heinrich, B. *J. Am. Chem. Soc.* **1998**, *120*, 9526.
(4) Enomoto, M.; Aida, T. *J. Am. Chem. Soc.* **2002**, *124*, 6099. (b) Enomoto, M.; Aida, T. *J. Am. Chem. Soc.* **1999**, *121*, 874. (c) Kawa, M.; Fréchet, J. M. J. *Chem. Mater.* **1998**, *10*, 286. (d) Issberner, J.; Vögtle, F.; Cola, L. D.; Balzani, V. *Chem. Eur. J.* **1997**, *3*, 706. (e) Tomoyose, Y.; Jiang. D.-L.; Jin, R.-H.; Aida, T.; Yamashita, T.; Horie, K.; Yashima, E.; Okamoto, Y. *Macromolecules* **1996**, *29*, 5236. (f) Newkome, G. M.; Guther, R.; Moorefield, C. N.; Cardullo, F.; Echegoyen, L.; Perezcordero, E.; Luftmann, H. *Angew. Chem., Int. Ed. Engl.* **1995**, *34*, 2023.

(5) Enomoto, M.; Kishimura, A.; Aida, T. *J. Am. Chem. Soc.* **2001**, *123*, 5608.
(6) Percec, V.; Glodde, M.; Bera, T. K.; Miura, Y.; Shiyanovskaya, I.; Singer, K. D.; Balagurusamy, V. S. K.; Heiney, P. A.; Schnell, I.; Rapp, A.; Spiess, H.-W.; Hudson, S. D.; Duan, H. *Nature (London)* **2002**, *419*, *384.* (b) Percec, V.; Ahn, C.-H.; Ungar, G.; Yeardley, D, J, P.; Möller, M.; Sheiko, S. *Nature* (*London*) **1998**, *391*, 161. (c) Yamaguchi, N.; Hamilton, L. M.; Gibson, H. W. *Angew. Chem., Int. Ed.* **1998**, *37*, 3275. (d) Schenning, A. P. H. J.; Elissen-Román, C.; Weener, J.-W.; Baars, M. W. P. L.; van der Gaast, S. J.; Meijer, E. W. *J. Am. Chem. Soc.* **1998**, *120*, 8199. (e) Hudson, S. D.; Jung, H.-T.; Percec, V.; Cho, W.-D.; Johansson, G.; Ungar, G.; Balagurusamy, V. S. K. *Science* **1997**, *278*, 449. (f) Lorenz, K.; Holter, D.; Stuhn, B.; Mülhaupt, R.; Frey, H. A. *Adv. Mater.* **1996**, *8*, 414. (g) Kim, Y.-H. *J. Am. Chem. Soc.* **1992**, *114*, 4947.
(7) Tomioka, N.; Takasu, D.; Takahashi, T.; Aida, T. *Angew. Chem., Int. Ed.* **1998**, *37*, 1531.
(8) Jang, W.-D.; Jiang, D.-L.; Aida, T. *J. Am. Chem. Soc.* **2000**, *122*, 3232.
(9) Marmillon, C.; Gauffre, F.; Gulik-Krzywicki, T.; Loup, C.; Caminade, A.-M.; Majoral, J.-P.; Vors, J.-P.; Rump, E. *Angew. Chem., Int. Ed.* **2001**, *40*, 2626.
(10) Partridge, K. S.; Smith, D. K.; Dykes, G. M.; McGrail, P. T. *Chem. Commun.* **2001**, 319.
(11) Kim, C.; Kim, K. T.; Chang, Y.; Song, H. H.; Cho, T.-Y.; Jeon, H.-J. *J. Am. Chem. Soc.* **2001**, *123*, 5586.
(12) Bellamy, L. J. *The Infrared Spectra of Complex Molecules*, 3rd ed.; Chapman and Hall: New York, 1975.
(13) Hanabusa, K.; Matsumoto, Y.; Miki, T.; Koyama, T.; Shirai, H. *J. Chem. Soc., Chem. Commun.* **1994**, 1401. (b) Porzi, G.; Sandri, S. *Tetrahedron: Asymmetry* **1994**, *5*, 453. (c) Ishida, Y.; Aida, T. *J. Am. Chem. Soc.* **2002**, *124*, 14017.
(14) Heinrich, B.; Praefcke, K.; Guillon, D. *J. Mater. Chem.* **1997**, *7*, 1363. (b) Lai, C. K.; Tsai, C.-H.; Pang, Y.-S. *J. Mater. Chem.* **1998**, *8*, 1355. (c) Kishikawa, K.; Furusawa, S.; Yamaki, T.; Kohomoto, S.; Yamamoto, M.; Yamaguchi, K. *J. Am. Chem. Soc.* **2002**, *124*, 1597.
(15) Kwon, Y.-K.; Danko, C.; Chvalun, S.; Blackwell, J.; Heck, J. A.; Percec, V. *Macromol. Symp.* **1994**, *87*, 103. (b) Kwon, Y.-K.; Chvalun, S.; Schneider, A.-I.; Blackwell, J.; Percec, V.; Heck, J. A. *Macromolecules* **1994**, *27*, 6129. (c) Kwon, Y.-K.; Chvalun, S. N.; Blackwell, J.; Percec, V.; Heck, J. A. *Macromolecules* **1995**, *28*, 1552.

MA034221B